Supporting Information

Sheline *et al.* 10.1073/pnas.0812686106

SI Text

Behavioral Data. The rating data acquired during the look condition was analyzed with a repeated measures ANOVA that included picture type (look negative, look neutral) as a within subject factor and diagnostic group (control, depressed) as a between subject factor. This analysis revealed a significant main effect of picture type ($F = 365.3$, d.f. = 1, 43, $P < 0.001$). Both groups rated the negative pictures as more negative than the neutral pictures in the look condition. There was no significant interaction with group ($F(1, 43) = 2.2$, $P = 0.14$). However, a posthoc analysis showed a trend for depressed subjects to rate negative pictures more negative than the control group ($t(43) = -1.79$, $P = 0.079$) in the look condition. The influence of regulation on responses to negative pictures was analyzed with a repeated measures ANOVA that included the different trial types for negative picture presentation (look, make positive, make negative) as a within subject factor and diagnostic group as a between subject factor. This ANOVA revealed a significant main effect of trial type ($F = 127.04$, d.f. = 2, 86, $P < 0.001$) because both groups rated pictures as most negative in the "make negative" condition and least negative in the "make positive" condition, with ratings in the look condition falling in between. There was no significant interaction with group ($F(2, 86) = 0.75$, $P = 0.477$).

Default Mode Network (DMN) for Regions of Interest (ROIs) Identification. To test our hypotheses, we identified a priori the DMN boundaries to determine ROIs in our data falling within the DMN by using standard methods (1). Specifically, three standard coordinates for default region seeds were used to generate resting state connectivity maps, and the average of these connectivity maps were applied in the current experiment. Distributed seed regions were comprised of 6-mm-radius spheres centered on published foci (1). DMN spheres were placed in medial prefrontal cortex (−1, 47, −4), posterior cingulate/precuneus (−5, −49, 40), and lateral parietal cortex (−45, −67, 36). The resulting connectivity map corresponds closely to published DMN maps from PET data (2, 3) and fMRI (1, 4) (Fig. 1).

The connectivity maps were defined in a separate healthy population and applied in the current experiment. Twenty healthy, right-handed, neurologically normal participants (10 women) aged 20 to 29 years (mean 25.5 ± 1.8) were recruited from the Washington University community and BOLD images were acquired during an eyes open resting state. Subjects were excluded if they had contraindications to MRI, history of mental illness, possible pregnancy, or medication use that could interfere with brain function. All experiments were approved by the Human Research Protection Office at Washington University in St. Louis. Written informed consent was provided by all participants.

These resting state functional connectivity data were temporally band-pass filtered ($f < 0.08$) and spatially smoothed (6-mm FWHM). Sources of spurious variance and their temporal derivatives were removed from this data through linear regression (5). Nuisance regressors included signals averaged over ventricle, white matter, and whole brain ROIs as well as measures of head movement. Correlation maps were produced by extracting the BOLD time course from the seed region and computing the Pearson's r between that time course and that of every other voxel in the brain. To combine results across subjects and compute statistical significance, correlation coefficients were converted to a normal distribution by Fischer's z transformation. Fischer z maps were combined across subjects by using a random-effects analysis (one sample t test, $n = 20$) and thresholded at $Z > 3.0$ ($P < 0.01$, cluster >17 voxels, corrected for multiple comparisons).

Stimulus Presentation. During the experiment, there were 4 runs of 24 trials each (96 trials). Each trial lasted 25.0 s, starting with instruction ("look", "positive", or "negative") presented for 2.5 s. Picture presentation followed for 10 s. After the picture, participants had 7.5 s to rate how they felt at that moment by using the hand-held button box: 0 = very positive; 1 = somewhat positive; 2 = neutral; 3 = somewhat negative; 4 = very negative. The word "relax" then appeared for 5 s until the onset of the next trial. Each run presented 6 trials in each condition, counterbalanced for picture type and instruction within and across runs and across subjects, to allow for estimates of bold responses to each trial type. Stimuli were from the International Affective Picture Series (6) based on the combined female and male valence and arousal ratings to produce 8 distinct sets of 6 neutral and 18 negative pictures.

Image Acquisition and Preprocessing. fMRI images were collected on a Siemens 3T Allegra MRI scanner by using an asymmetric spin-echo echo-planar sequence with volume repetition time (TR) = 2.5 s (slice TR = 64.10 ms), echo time (TE) = 25 ms, flip angle = 90°, and field of view = 205 cm. One acquisition consisted of 39 transverse slices, 3.2 mm thick (no gap), and in-plane resolution = 3.2 × 3.2 mm. Each functional run began with 4 volume images that were not analyzed, followed by 246 acquisitions for the paradigm. High-resolution structural images (MPRAGE) (1 × 1 × 1.25 resolution) used a sagittal 3D T1-weighted sequence (TR = 1.9 s, TE = 3.93 ms, flip angle = 7°, and TI = 1000 ms). The task-related functional imaging data were preprocessed to correct for asynchronous slice acquisition and odd/even slice intensity differences caused by interleaving. Data were rigid body motion corrected, atlas transformed (12 parameter affine) via the structural images by using a representative target image (7), and resampling to 3-mm isotropic voxels. Before statistical analysis, the data were smoothed by using a 9-mm FWHM Gaussian filter.

Image Analysis. For each participant, a general linear model was used to estimate hemodynamic model-independent event related responses over 35 s (14 frames to cover the 20 s of the trial plus and an additional 15 s for the evolution of the homodynamic response) with a separate estimate for each of the task conditions. The first 8 frames were used for this analysis, which should reflect BOLD responses related to picture viewing and emotion regulation when one takes into account the lag in the hemodynamic response. ROIs were identified as falling within the DMN as described above in *Default Mode Network for Regions of Interest Identification*.

Exploratory Effects. To look for nonpredicted effects in regions outside the a priori DMN ROI, we conducted exploratory analysis to ensure that we had not inadvertently omitted important group effects outside the DMN. We conducted a whole-brain ANOVA to determine group main effects or interaction with group. The ANOVA results were thresholded to obtain an uncorrected whole-brain, false-positive rate of 0.05 (corrected $P < 0.0001$) and a minimum-cluster extent of 14 or more

contiguous voxels. We found 4 regions in the cerebellum in which depressed subjects had less of a decrease in activity (group X time effect) than controls. These regions were in the cerebellar tonsils (−3, −42, −30), left rostral cerebellar vermis (−10, −52, −18), and two regions in the right lateral cerebellum (39, −71, −24) and (49, −46, −27). These four regions had decreased activity in response to both negative pictures and attempting to regulate emotional responses in controls. In these same regions, depressed subjects had less of a decrease in activity. There are two interesting aspects of this finding. The first is that the cerebellar tonsils, where one of the regions showing group differences was located, may actually be part of the DMN (8). The second is that recent evidence implicates the cerebellum in emotional processing, including the demonstration of functional and structural abnormalities in depression (9–11).

1. Fox M, *et al.* (2005) The human brain is intrinsically organized into dynamic, anticorrelated functional networks. *Proc Natl Acad Sci USA* 102:9673–9678.
2. Shulman G, *et al.* (1997) Common blood flow changes across visual tasks II: Decreases in cerebral cortex. *J Cogn Neurosci* 9:648–663.
3. Buckner R, Andrews-Hanna J, Schacter D (2008) The brain's default network: Anatomy, function, and relevance to disease. *Ann NY Acad Sci* 1124:1–38.
4. Fox M, Raichle M (2007) Spontaneous fluctuations in brain activity observed with functional magnetic resonance imaging. *Nat Rev Neurosci* 8:700–711.
5. Biswal B, Yetkin F, Haughton V, Hyde J (1995) Functional connectivity in the motor cortex of resting human brain using echo-planar MRI. *Magn Reson Med* 34:537–541.
6. Mayberg H (1997) Limbic-cortical dysregulation: A proposed model of depression. *J Neuropsychiatr and Clin Neurosci* 9:471–481.
7. Talairach J, Tournoux P (1988) *Co-Planar Stereotaxic Atlas of the Human Brain* (Georg Thiem Verlag, Stuttgart).
8. Vincent J, *et al.* (2007). Intrinsic functional architecture in the anaesthetized monkey brain. *Nature* 447:83–86.
9. Snider R, Maiti A (1976) Cerebellar contributions to the Papez circuit. *J Neurosci Res* 2:133–146.
10. Schmahmann J, Anderson C, Newton N, Ellis R (2001) The function of the cerebellum in cognition, affect and consciousness: Empirical support for the embodied mind. *Conscious Emotion* 2:273–309.
11. Schutter D, van Honk J (2005) The cerebellum on the rise in human emotion. *The Cerebellum* 4:290–294.

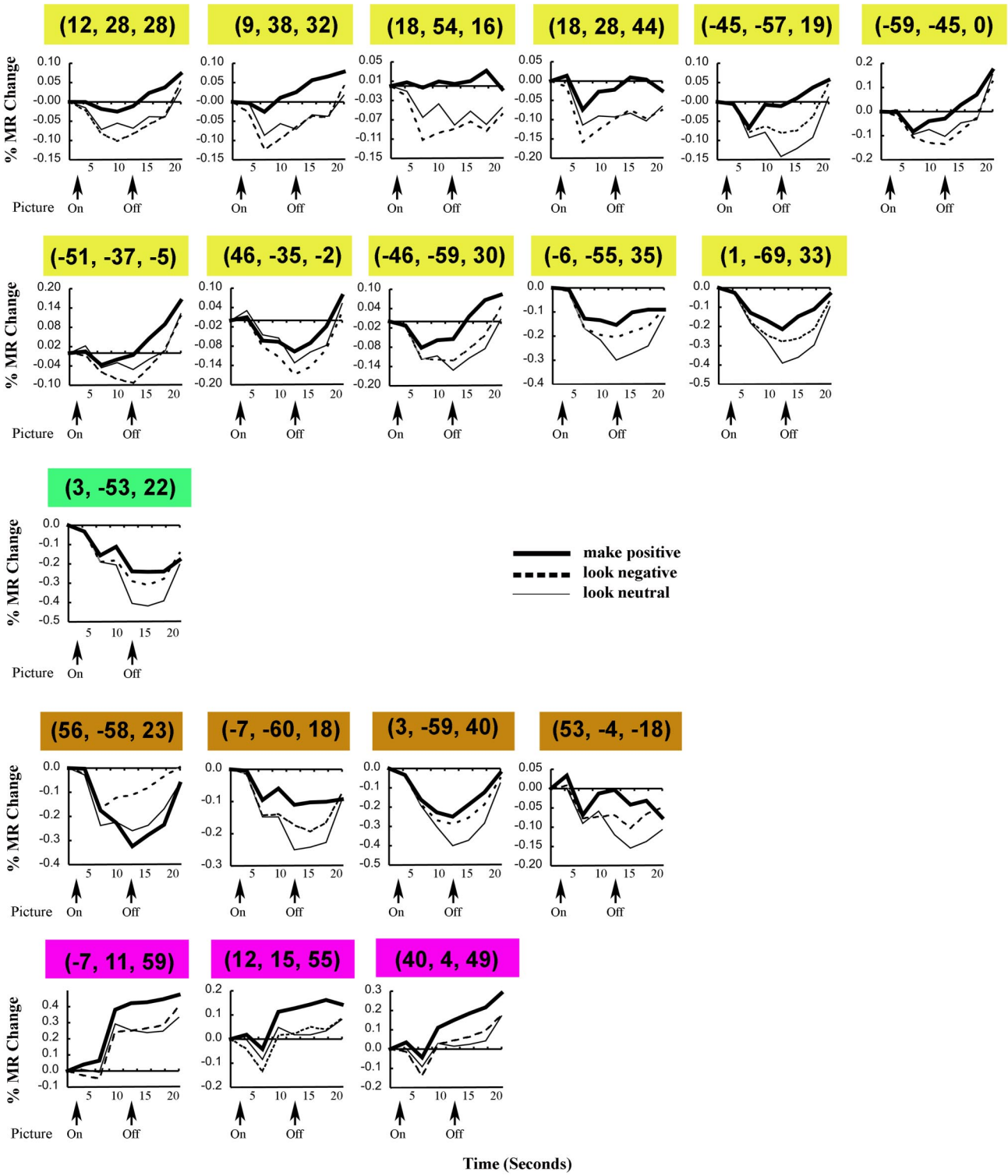

Fig. S1. Time–activity curves are shown for the subset of regions not displayed in Figure 2 (see Table 1). Time–activity curves plot percent fMRI signal change (*y* axis) vs. time in seconds (*x* axis). Regions compare passive viewing of negative pictures to passive viewing of neutral pictures (look) (first row) and compare passive viewing of negative pictures to regulation of emotion (regulate) and time within trial that reflected modulations of task-related activation (fourth row). As indicated, there were differences in activity in depressed compared with control subjects in the look (first row) and regulate conditions (second row) in left medial BA8, right dorsal BA32, right medial frontal BA10, and right lateral parietal cortex. In addition, there were differences in activity in depressed compared with control subjects in the look condition (third row) and regulate conditions (fourth row) in 4 left lateral temporal cortex regions.

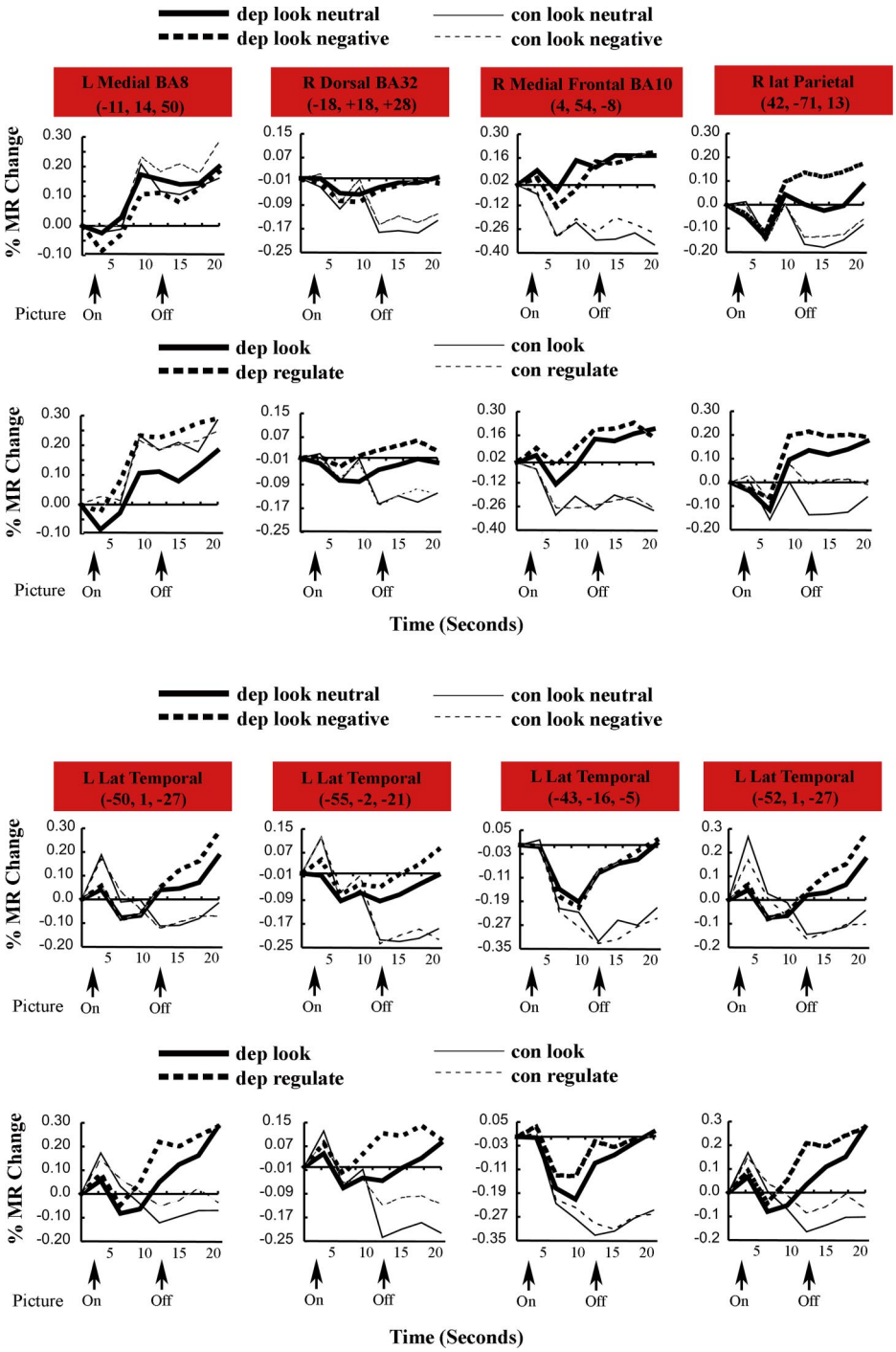

Fig. S2. Time–activity curves are shown for regions without group effects (see Table S1). Colors and coordinates indicate the regions and effects shown in Figure 1. Time–activity curves plot percent fMRI signal change (*y* axis) vs. time in seconds (*x* axis). The combined depressed and control subjects were used to compare passive viewing of negative pictures (look negative) vs. passive viewing of neutral pictures (look neutral) vs. regulation of emotion (make positive) and time within trial that reflected modulations of task-related activation. As indicated, there were regions that had no group differences but had activity decreases in the regulate condition only (make positive vs look negative) (yellow), activity decreases in the look condition only (look neutral vs look negative) (green), decreases in both the regulate and look conditions (brown), or activity increases in both the regulate and look conditions (fuschia).

Table S1. Regions showing significant activations in the look and regulate effects but no group differences

Regions	(X, Y, Z)	No. of voxels	Look effect value	Regulate effect value
Decreased activity				
Cingulate/medial dorsal prefrontal cortex				
Rostral BA32	12, 28, 28	99	ns	<0.001
Dorsal BA9	9, 38, 32	113	ns	<0.001
Superior frontal BA10	18, 54, 16	114	ns	<0.001
Superior frontal BA8	18, 28, 44	106	ns	<0.001
Lateral parietal/temporal cortex				
BA22	−45, −57, 19	107	ns	<0.001
BA21	−59, −45, 0	121	ns	<0.001
BA21	−51, −37, −5	127	ns	<0.001
BA21	46, −35, −2	82	ns	<0.001
BA40	−46, −59, 30	121	ns	<0.001
BA40	56, −58, 23	141	<0.001	<0.001
Posterior cingulate/precuneus				
Posterior cingulate BA31	−7, −60, 18	245	<0.001	0.01
Posterior cingulate BA30	3, −53, 22	143	<0.001	ns
Precuneus BA7	3, −59, 40	139	<0.001	0.004
Precuneus BA31	−6, −55, 35	125	ns	<0.001
Precuneus BA7	1, −69, 33	224	ns	<0.001
Orbital gyrus				
Gyrus rectus BA11	53, −4, −18	70	<0.001	0.01
Increased activity				
Medial superior frontal BA6	−7, 11, 59	133	<0.001	<0.001
Superior frontal BA6	12, 15, 55	118	<0.001	<0.001
Superior frontal BA8	40, 4, 49	122	<0.001	<0.001